A Solid-Inclusion Borehole Probe to Determine Three-Dimensional Stress Changes at a Point in a Rock Mass

GEOLOGICAL SURVEY BULLETIN 1258-C

A Solid-Inclusion Borehole Probe to Determine Three-Dimensional Stress Changes at a Point in a Rock Mass

By THOMAS C. NICHOLS, JR., JOHN F. ABEL, JR., *and* FITZHUGH T. LEE

CONTRIBUTIONS TO ENGINEERING GEOLOGY

GEOLOGICAL SURVEY BULLETIN 1258-C

Development and laboratory testing of a solid-inclusion borehole instrument and the mathematical bases for reduction of the three-dimensional data produced by the instrument

UNITED STATES GOVERNMENT PRINTING OFFICE, WASHINGTON : 1968

UNITED STATES DEPARTMENT OF THE INTERIOR

STEWART L. UDALL, *Secretary*

GEOLOGICAL SURVEY

William T. Pecora, *Director*

For sale by the Superintendent of Documents, U.S. Government Printing Office
Washington, D.C. 20402 - Price 15 cents (paper cover)

CONTENTS

ILLUSTRATIONS

NOTE

In this report a theoretical cylinder was used for the elastic approximation of a spherical inclusion in an elastic epoxy host. The actual theoretical spherical approximation for a rigid sphere in a semi-infinite mass of low-modulus material produces a stress concentration factor of about 1.9 instead of the 1.5 factor for a rigid cylinder (Goodier, 1933, p. 40; Edwards, 1951, p. 26–27). The apparent cause of this higher stress concentration factor is the lack of as much adjacent rigid material to distribute the available stress.

It must be understood that no complete theoretical three-dimensional elastic analysis exists for the exact case of the probe in rock, because (1) the probe is surrounded by only one diameter of low-modulus material across the borehole and 6½ diameters along the borehole and (2) no rock mass rigorously meets the requirements of isotropy and homogeneity required for the application of theoretical elasticity.

An approximate theoretical elastic solution is possible by combining the results of two plane strain analyses, one across the borehole and one along the borehole. This can be done, using the finite element technique.

A SOLID-INCLUSION BOREHOLE PROBE TO DETERMINE THREE-DIMENSIONAL STRESS CHANGES AT A POINT IN A ROCK MASS

By THOMAS C. NICHOLS, Jr., JOHN F. ABEL, Jr., and FITZHUGH T. LEE

ABSTRACT

In order to relate changing stress conditions within rock masses to geologic factors, a welded high-modulus solid-inclusion borehole probe to determine three-dimensional stress changes at a point in a rock mass was developed and tested.

The probe consists of a 1-inch-diameter chrome alloy steel ball, mounted with three strain-gage rosettes, and is encapsulated in a filled waterproof epoxy. The reliability of the probe is established by conducting a series of tests in which the probe was subjected to changing hydrostatic and triaxial stress fields. In all these tests the probe responded as predicted by elastic theory.

Because reduction of field measurements is difficult and time consuming by use of a desk calculator, computation of the three-dimensional stress tensor has been programed for computer analysis.

The probe, when adequately field tested, will be capable of resolving data that will aid in the understanding of anisotropic rock behavior associated with tunneling and other underground or near-surface engineering operations.

INTRODUCTION

The U.S. Geological Survey started research in July 1965 on the behavior of rock masses under changing stress conditions caused by the excavation of underground openings.

The natural stress field that exists at a point within a rock mass, prior to any excavation, is dependent on the depth below the surface and the physical characteristics of the medium. The physical characteristics of a rock mass are affected by all the geologic processes to which it has been subjected. Geologic processes may produce folding, fracturing, faulting, jointing, chemical alteration, recrystallization, foliation, lineation, and other rock anisotropies. Changes in the preexisting stress field at any point in a rock mass, which result from excavation, are controlled by the physical characteristics of the rock mass, the proximity of the point of measurement to the excavation, and the geometry of the excavation.

Theoretical methods have been developed for estimating the stress distribution near different types of excavations within an idealized elastic body (Obert and others, 1960, p. 8–29). However, field investigations and measurements of rock strains have demonstrated that divergencies from elastic theory occur in even the most elastic rock masses (Obert, 1962, p. 8; Merrill and others, 1964, p. 32–37; Dare, 1962, p. 16; Utter, 1962, p. 17–19; Hast, 1958, p. 74–79; Panek and Stock, 1964, p. 50–52; Wisecarver and others, 1964, p. 12–20; Morgan and others, 1965, p. 45–47; and Ryder and Officer, 1965, p. 182–188). This suggests that most rock masses are less competent, less homogeneous, and behave less elastically than the idealized models used in theoretical investigations, many of which are based on laboratory physical property measurements of small samples (Leeman, 1964, p. 82–114). It is reasonable to assume that the greater the deviation of a rock mass from a perfectly elastic material, the greater will be the deviation of its behavior from that predicted by elastic theory. The stress conditions that exist adjacent to an excavation within a fractured rock mass cannot be estimated with confidence by any existing technique. Consequently, most past measurements have been made under the most favorable geologic conditions in relatively homogeneous media such as massive granite, gneiss, rock salt, trona, magnetite, anhydrite, and thick-bedded sandstone.

The problem of measuring the actual stress changes that are induced in the rock surrounding an underground opening has intrigued and challenged many investigators. Efforts to make measurements of these stress changes in natural materials and on full-size underground structures have been largely unsuccessful until the last decade because of the lack of suitable instrumentation.

The availability of new instrumentation (Hast, 1958) has permitted the approximate determination of the rock stresses acting in the plane perpendicular to the axis of an instrumented borehole. Analysis of these stresses required the assumptions of (1) isotropy, (2) perfect elasticity, and (3) either plane stress or plane strain. Subsequent developments have made it possible to measure the degree of anisotropy and the variations of the elastic moduli of the rock at the point where the instrumentation has been applied (Fitzpatrick, 1962). Although the necessity for assuming plane stress or plane strain has not been eliminated in any previous methods of instrumentation and interpretation, the theoretical works of Sechler (1952) and Panek (1966) have shown that these assumptions are not required; thus these assumptions will undoubtedly be eliminated in the future.

The mathematical analysis of stress changes induced around openings in theoretically elastic bodies has been accomplished (Goodier,

1958) assuming either plane stress or plane strain. The planar analysis assumes that the opening can be represented by a slice (plane) of effectively infinite extent in two directions and of finite (negligible) extent in the direction of the long axis of the opening. The plane stress approximation assumes that the slice is subjected to no restraint in the direction of the opening axis when stresses are applied in the plane. The plane strain approximation assumes that all strain in the direction of the opening is prevented as stresses are applied in the plane. These analyses have provided the basic background for predicting stress levels which can be anticipated in rock surrounding underground structures.

Two possible methods of instrumentation to eliminate the necessity of assuming plane stress or plane strain in interpreting measurement data have been proposed (Panek, 1966; Leeman, 1964): (1) Measure the extension of the borehole as well as the diametrical change resulting from three-dimensional stress changes, and (2) measure the diametrical borehole change at the point under investigation in two or more boreholes with different bearings and inclinations. The first method was used in the present investigation because of the difficulty of accomplishing the second. Prior to construction of the probe described in this paper, instrumentation for the first method was not available. For this instrumentation two types of probes may be constructed—one of low-elastic-modulus material and the other of high-elastic-modulus material. Both types of probes may be used successfully to determine plane strain; however, because of the probability of the instrument being disturbed by shock waves, the low-modulus type is not practical for investigating stress changes around an active underground opening being excavated by explosives. Consequently, a high-modulus instrument grouted in a drill hole was developed for use in the present investigation. High-modulus instrumentation also eliminates the need for accurately determining the anisotropic variation of rock strength and modulus provided that the instrument modulus is approximately five times greater than the rock modulus (Leeman, 1964, p. 61); such a high-modulus instrument effectively acts as a rigid inclusion in the medium.

Stresses in an ordinary jointed or faulted rock mass are universally compressive within the earth. Tensile stresses cannot be transmitted across breaks in a rock mass, but relative tensile strains can be produced and measured. These strains result either from decreases in compression as the opening is approached or from Poisson strain in a plane normal to the direction of an increased compressive stress.

The main objective of the investigation was to use the high-modulus three-dimensional borehole probe to monitor the stress changes around an active underground opening during excavation. It was believed

that by use of these measurements, together with geophysical and conventional rock mechanics measurements, relationships could be established that would provide a basis for making accurate predictions of the behavior of a rock mass during tunnel construction. With such predictions, more efficient and economical tunnel support (temporary and permanent) could be installed as a tunnel was being driven.

Although the following discussion is concerned primarily with a solid-inclusion probe for use in rock, a similar probe for installation in soil and intensely altered rock masses (for example a fault gouge) is currently being developed in the laboratory. It is anticipated that such a probe will be valuable for determining the three-dimensional stress field changes associated with landslides, building foundation materials, earthfill dams, and many engineering-construction projects.

SCOPE OF INVESTIGATION

The long-range objectives of this investigation are (1) to determine the three-dimensional changes in the stress field that occur in a rock mass when a part of that rock mass is excavated and (2) to determine how geologic conditions alter or influence these stress changes. The initial laboratory phases of probe development, calibration, and model studies have been completed and are reported here. Preliminary measurements of the three-dimensional stress changes are presently being made in a rock mass close to an active underground excavation. These measurements permit the determination of stress changes around the excavation. The magnitude, direction, and location of stress concentrations resulting from the excavation are being obtained. This information by comparison makes it possible to determine how the theoretical elastic stress pattern adjacent to the excavation has been altered by the geologic conditions at the test location.

The probe described here can be employed over a wide range of geologic conditions, grossly unsuited to existing low-modulus stress determination instrumentation, because it is designed so that measurements can be made in the presence of joints, foliation or bedding, and lithology—anisotropies that weaken a rock mass. The probe is designed to average out the variations in rock mass characteristics, competency, and anisotropy.

INSTRUMENTATION

PROBE DEVELOPMENT

The first step in developing the high-modulus three-dimensional borehole probe was to review the results of related studies made by previous investigators.

A search of the literature revealed that a probe having the desired capabilities had not been constructed previously. According to Leeman (1964, p. 54–55), a probe capable of monitoring strain for determination of stress changes within a material would have the following characteristics. It would consist of an effectively rigid, ideally elastic material. The probe would have strain-sensing devices oriented so as to obtain complete information on the magnitudes and directions of the principal stresses acting on it. The probe would be welded as an inclusion into the host material so that any changes of stress in the host material would be accompanied by proportional stress changes acting in the same direction in the probe. The strain changes induced in the probe should be large enough to be measured accurately. If the modulus of the probe material is approximately five times that of the host material, stress changes in the probe can be expected to be as much as 2 times those in the host material.

The geometry of the probe and the boundary conditions that affect the stress distributions were important factors that had to be considered in the development of the borehole probe.

Two geometric forms, the cube and sphere, were thought to be the best possible choices for the strain-sensing elements. The cube was considered because orthogonal planes necessary for determining a three-dimensional stress field (Leeman, 1964, p. 49) are defined by the sides of the cube and because strain instrumentation of these sides is very easily achieved. However, anomalous stress distributions located at the edges and corners of the cube, as well as possible distortion of transmitted stresses across the edge boundaries, discouraged its use. The sphere does not have orthogonal planes on which to mount strain-sensing devices, but it has the advantage that stress distribution is relatively uniform and free of directional distortion. The stress level in the spherical probe would be greater than that in the host medium because of the difference in stiffness (modulus) between the two materials. As previously stated, small changes in the modulus of the host medium are of little consequence provided the probe modulus remains at least five times greater than the modulus of the rock mass.

For a high-modulus inclusion, welded to the host material, the strain in a given direction at the center of the sphere is equal to the strain measured in the same direction at a point on the surface of the sphere (Edwards, 1951, p. 26). Therefore, strain-measuring devices (strain-gage rosettes) can be placed on a sphere in such a manner that the strain components in orthogonal planes can be determined.

An error is introduced because the strain gages occupy a finite area on the surface of the sphere, instead of a point as postulated by the theory. However, the magnitude of this error is less than 1 percent for

the 1-inch ball and ⅛-inch strain gages. This small error is eliminated in the hydrostatic calibration step.

In order to resolve the magnitude and direction of the stress changes in the three-dimensional stress field at a point within a material, it is necessary to know six components of the stress tensor (Leeman, 1964, p. 48). Of these components, three are the normal stresses acting perpendicular to mutually orthogonal planes and the other three are the shear stresses acting on the same orthogonal planes. Thus strain-sensing devices must be placed on the probe so that these six components of stress can be calculated from strain measurements. The strain of the sphere can then be used to calculate the stress in the adjacent rock.

As a result of the previous consideration it was decided to design and construct a spherical probe with three strain-gage rosettes mounted orthogonally on the surface of the sphere. The three strain-gage rosette sensors represent planes tangent to the probe and are normal to a set of three orthogonal axes. These normals have been given the designation of x, y, and z, and are called the reference axes. The z axis is coincident with the borehole axis and is normal to the plane tangent to rosette 3, the x axis is parallel to the normal of the plane tangent to rosette 2, and the y axis is parallel to the normal of the plane tangent to rosette 1 (fig. 1). Because of this particular orientation of the rosettes, two strain gages on each rosette are parallel to two of the reference axes.

One rosette could have been eliminated if strain measurements had been made by two nonorthogonal rosettes placed on the probe. The theoretical basis for this simplified technique is presented in detail by Panek (1966). Difficulties encountered in the field application of this technique (Wentworth, 1966) and the lack of redundancy of strain measurements used to check the normally directed strains induced the present authors to employ the three-rosette system.

The detailed mathematical analysis begins on page C19.

For the core of the probe, a 1-inch-diameter chrome alloy steel ball bearing (sphere) was used. These balls have a roundness tolerance of less than 0.0005 inch and an elastic modulus of 30.5×10^6 psi (pounds per square inch). The balls were first etched in a dilute solution of nitric acid to prepare the surface for epoxy bonding agents and also to check the surface for structural homogeneity. Then, the balls were cleaned with acetone to remove grease and foreign substances which could hinder bonding action of epoxies. Strain-gage rosettes consisting of three strain gages, 45° apart, were applied to the balls with an epoxy adhesive. Three rosettes were applied to each ball with the centers of the rosettes 90° apart as shown in figure 1. Electrical connections to the gages were made with 10-inch lengths of enamel-insulated copper wires. A cast acrylic rod approximately 8 inches long, used as a

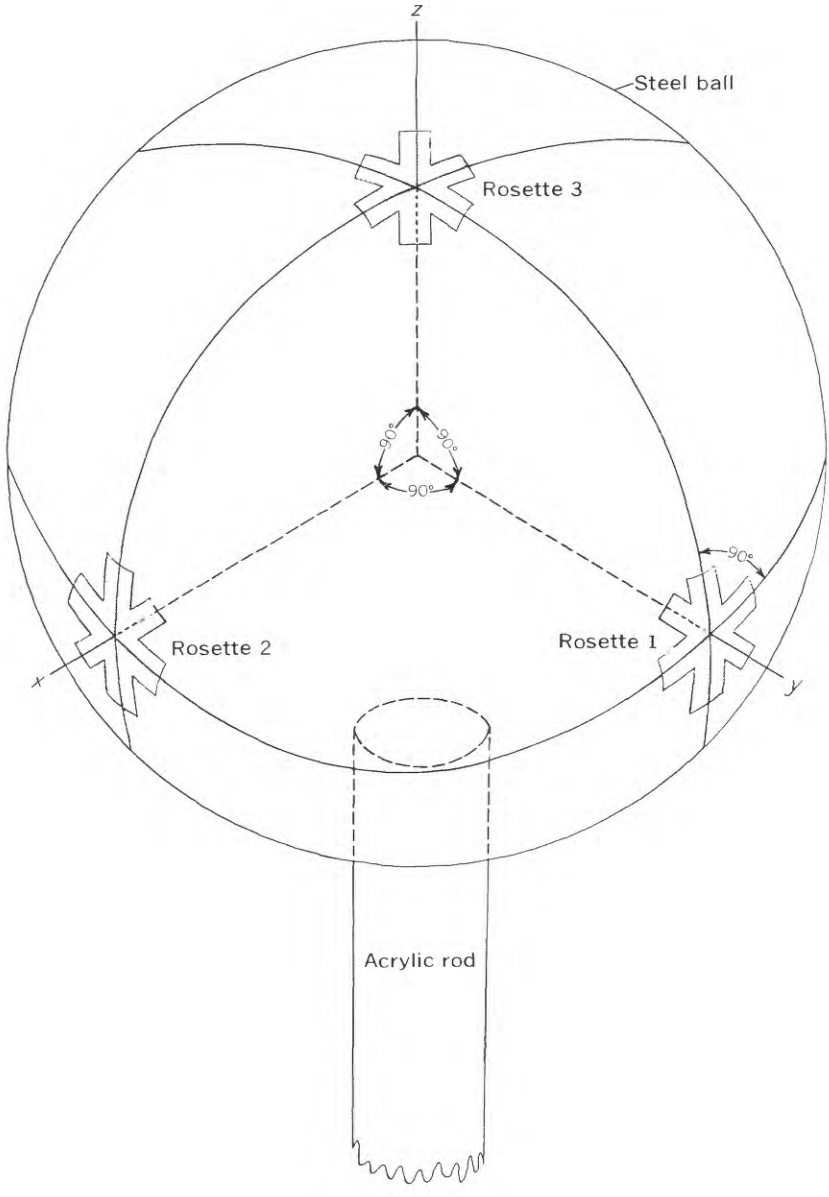

FIGURE 1.—Position of strain-gage rosettes on steel ball.

handle, was cemented to the ball with epoxy. Then the entire ball, with mounted gages and extending wires and handle, was sealed in a cylindrical capsule of epoxy grout approximately 1½ inches in diameter and 1⅝ inches high (fig. 2). The probe was then ready for testing.

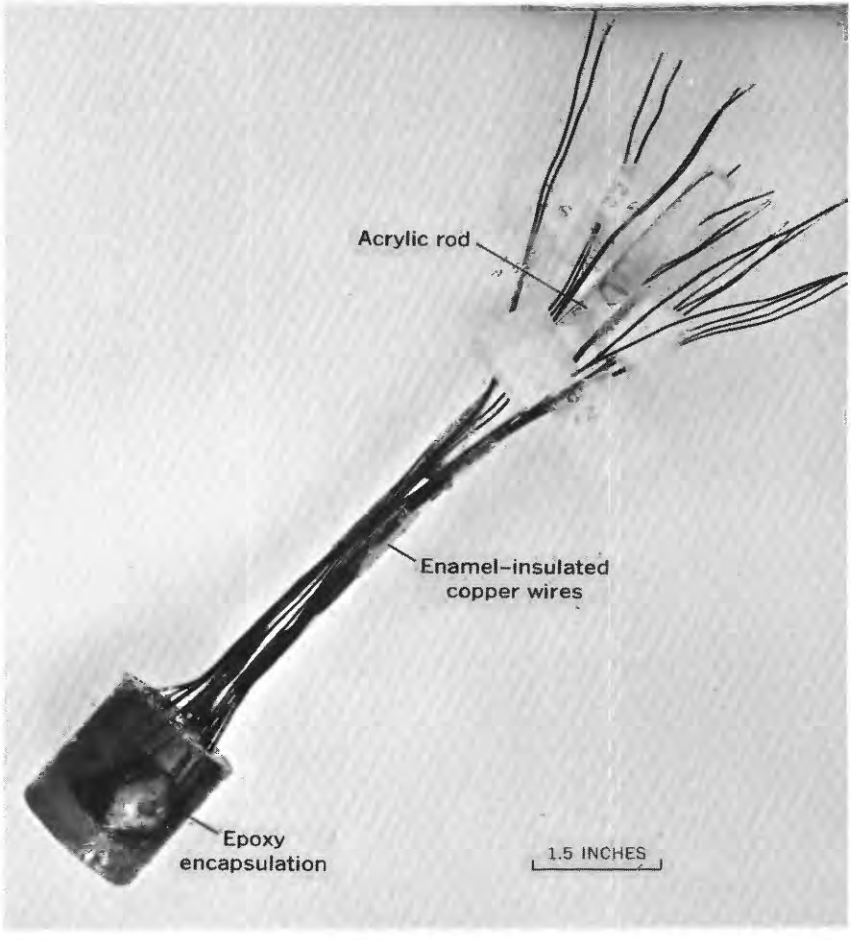

FIGURE 2.—Encapsulated three-dimensional borehole probe.

MONITORING SYSTEM

For testing in the laboratory, it was necessary to develop a monitoring system that would simultaneously and continuously measure the responses of as many as 27 strain gages. Several racks of strain-gage amplifiers, power supplies, and two-axis (x–y) recorders were used to provide a multichannel monitoring system that gave automatic recording of strain responses within the specimens being tested. The essential elements of this system are shown in figure 3.

For field tests, an ordinary battery-operated strain indicator, which is portable and easy to use and avoids the common problem of fluctuat-

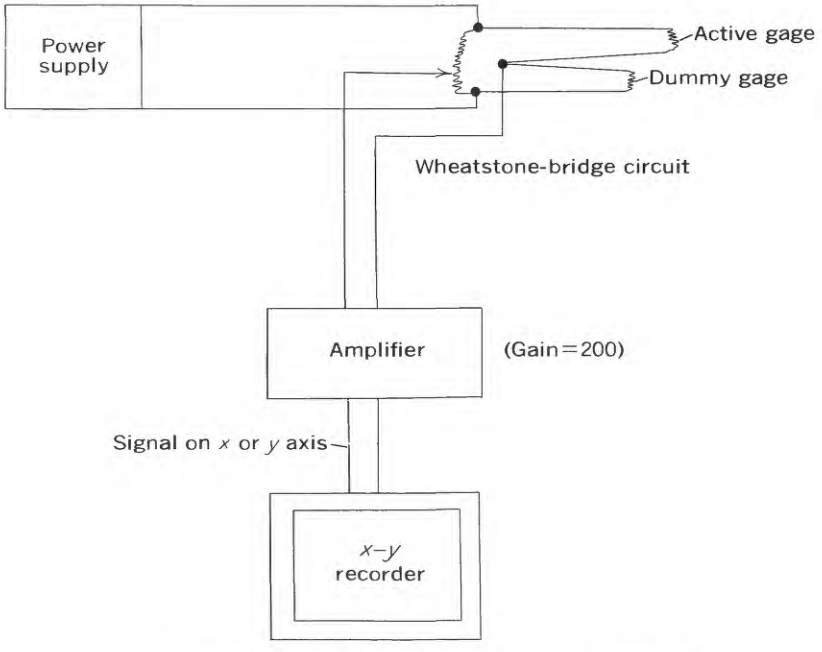

FIGURE 3.—Diagram of laboratory strain-monitoring system.

ing 110-volt alternating-current power in tunnels, was selected. The disadvantages of using this type of instrument are:

1. Only single readings can be taken, thus a switching device must be used to take all the readings at one station.
2. Because continuous readings cannot be taken, some stress anomalies may be missed if they do not exist at the time of scheduled readings.

Even with these readout disadvantages, enough information is being obtained to evaluate the effectiveness of the solid inclusion probe as a stress monitoring device.

GROUT

One of the practical problems which had to be solved as part of the development of the three-dimensional borehole probe was the formulation of a satisfactory grout. It was considered desirable, in order to minimize boundary effect errors, to use the same type of grout to encapsulate the probe and to couple the capsule to the host medium. Consequently, the following requirements were established:

1. The grout must act either as a rigid inclusion or as a low-modulus inclusion when placed in the drill hole.

2. The grout must form a high tensile strength bond between itself, the rock mass, and the probe.
3. The grout must behave elastically over the range of anticipated stress changes.
4. The grout must be virtually free of creep over the anticipated range of loading.
5. The grout must be waterproof in order to achieve electrical insulation of the probe.
6. The grout must exhibit a minimum amount of volume shrinkage during the curing period.

STIFFNESS

In order for the grout plug to act as a rigid inclusion between the probe and the rock mass it must be characterized by a stiffness (rigidity) of about five times the rock mass stiffness. The stiffness determined for rock specimens taken from various field test sites reached a level of strain of 6 psi per μin. per in. (pounds per square inch per microinch per inch). Field measurements from one of the test sites indicate that the stiffness of the rock mass does not exceed 2 psi per μin. per in. and generally is much lower because of geologic weakness of the rock mass not present in prepared laboratory specimens. Therefore, a stiffness on the order of 10 psi per μin. per in. was considered adequate for the grout.

Epoxy grouts of various formulations were tested in an extensive laboratory testing program. The stiffnesses of the unfilled (pure) epoxy materials tested were in the range of 0.3 to 0.4 psi per μin. per in. The addition of steel, carborundum, and fused alumina fillers to the epoxy generally resulted in increased stiffness. The maximum stiffness obtained was 1.5 psi per μin. per in. It was concluded that a grout plug sufficiently rigid to satisfy the requirements of a high-modulus bond could not be obtained by use of a pure epoxy or an epoxy-base grout. A filled epoxy grout, however, would satisfy the requirements of a low-modulus bond between the probe and the rock mass.

A requirement for a low-modulus grout is that the approximate stiffness of the grout and of the rock mass be known. This requirement can be met by either filled or unfilled epoxy materials.

Other observations made during the laboratory grout-testing program showed that:

1. Excessive air bubbles that were entrapped by the steel-filled epoxy decreased the stiffness.
2. Angular particles (crushed carborundum) resulted in higher stiffness and viscosity than rounded particles (fused alumina).

3. Grout viscosity decreased as the particle-size range of the fillers was successively restricted.
4. Introduction of only 3 percent minus 325-mesh particles drastically reduced the grout stiffness.

The actual selection of grout formulation should be made only after the conditions of emplacement have been completely evaluated. In any case, the selection of an optimum grout formulation would require the maximum stiffness attainable.

TENSILE STRENGTH

The tensile bond formed by the various epoxy grouts exceeded the tensile strength of the glass in the glass vials used to form the test specimens (fig. 4). This was true even when the surface of the vial was purposely dirtied in an effort to determine the influence of debris on the rock surface of a borehole. The epoxy appears to have the ability to absorb rock particles and to penetrate thin films of grease and oil.

The laboratory study included testing of grout under wet conditions as well as dry conditions. The field conditions will undoubtedly be damp, if not wet; therefore an acceptable grout must function properly under water.

ELASTIC RANGE

The elastic response of the various grouts was tested in the range of compression 1,500 to 7,000 psi. A rigid grout must be capable of transmitting the anticipated field stress changes of as much as 4,000 psi and strains of 2,000 μin. per in. (microinches per inch). A low-modulus grout, on the other hand, must be capable of transmitting strains of 2,000 μin. per in. The laboratory grout program has demonstrated that the requirements for a low-modulus grout, which we anticipate employing in the field investigations, are not difficult to achieve.

CREEP PROPERTIES

The grout presently being used has been tested for a period of 6 months under a constant static load and without a load. Temperatures have been allowed to vary as much as 7°F. Over this period there has been virtually no creep caused by loading. The only changes in strain which were recorded were in response to temperature changes and were attributed to thermal expansion and contraction.

ELECTRICAL INSULATION CHARACTERISTICS

The various epoxies with no fillers all had good insulating characteristics. However, the epoxy grouts with metal fillers lost most of their insulating characteristic when highly stressed. This indicates

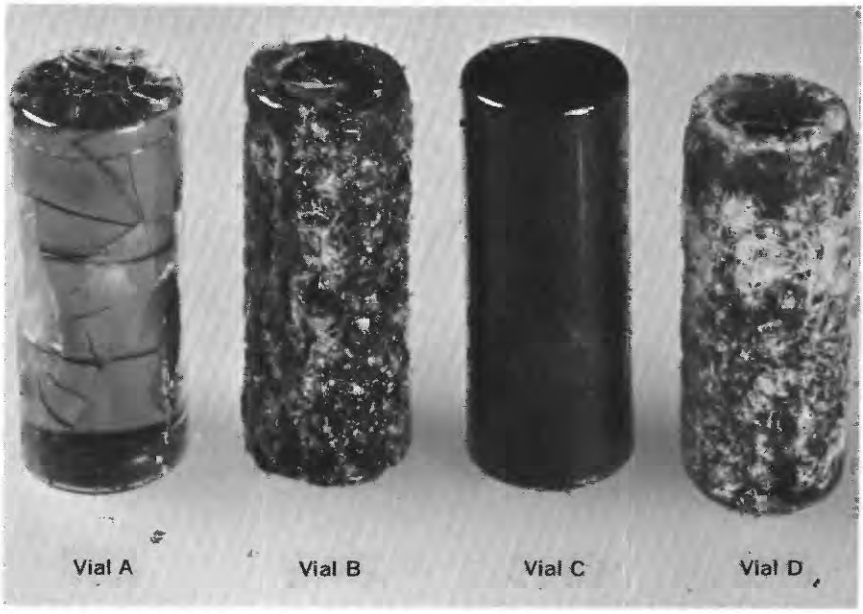

FIGURE 4.—Glass vial molds with cured epoxy casts. Molds are ¾ inch in diameter and 2 inches long. Vials A and D: Epoxy containing no filler. Vials B and C: Epoxy containing carborundum filler. No attempt was made to remove the glass from vials A and C, and curing stresses caused extensive fracture of vial A. An attempt was made to remove the glass from vials B and D, and the effect of high bond strength is apparent.

that the filling aggregate develops increased grout stiffness by making physical contact between the filling particles. This property tends to rule out the use of an epoxy with metal filler in contact with the probe. The use of strain gages requires a minimum of 50-megohm resistance to ground. The resistance to ground of partly-metal-filled grouts in contact with the probe was only about 100 ohms when stressed close to failure. The actual resistance depends on both the formulation of the epoxy and the stress level. The epoxy formulation with carborundum filler and fused silica filler developed resistance well above the 200-megohm level and maintained it under stress.

TESTING

HYDROSTATIC PROGRAM

In order to adequately calibrate the probe, encapsulated as shown in figure 2, and to determine if it was behaving in an essentially elastic manner, it was first tested in a hydrostatic stress field under varying stress increments and durations.

Each probe was placed in a triaxial chamber capable of withstanding pressures of 8,000 psi. The probe was then subjected to the following series of hydrostatic pressure tests.

Initially the pressure was increased in increments of 500 psi up to 2,500 psi. The 2,500-psi stress level was chosen as a maximum test pressure because it seemed doubtful that changes of stress more than 2,500-psi compression would occur within the rock at any of the potential field test sites. The pressure was then dropped back to 0 psi in one increment.

The resulting strains of pairs of the sensing elements of the strain-gage rosettes were automatically plotted on x–y recorders. Thus, the line plot on each x–y recorder represented the strain of two strain gages plotted against each other. If the probe was behaving in an elastic manner and if each strain gage was perfectly applied to the sensing sphere, a straight 45° line would be plotted. The x–y plots of the gages on all the probes tested so far have been straight-line plots having slopes very close to 45°. Slight deviations from 45° probably are caused by the strain gages not conforming precisely to the curvature of the ball, thus a small error is introduced in the strain response. Since the stress-strain ratio of the probe is known, it is a simple matter to correct for this error by calibrating each gage in a hydrostatic stress field.

Another test was performed on one probe to test the ability of the probe to accurately measure stress changes over a long period of time. The probe was placed in the triaxial chamber and the stress was raised to 2,000 psi by 500 psi increments. The probe was then allowed to remain under this stress for 2 weeks. Once each day during this period the stress was reduced to 0 psi and then returned to the upper limit to see if the gage calibrations remained constant and if the x–y plots were repeatable. Over the entire 2-week period the probe behaved in a uniform and repeatable manner.

A third hydrostatic test was performed on one probe to find the approximate stress at which the epoxy encapsulation would fail. The probe was placed in the triaxial cell and subjected to pressure in increments of 500 psi until failure occurred at 4,500 psi. Failure was presumably caused by high stress concentrations on the surface of the probe. After failure, the probe continued to record stress changes but the x–y plots were no longer linear in any range of stress application. Thus the probe is of no apparent value if the encapsulation material fails.

After the favorable performance of the probe in a hydrostatic stress field, the next step was to test it in a uniaxial or triaxial stress field to further determine its elastic behavior. This was done by grouting

it in a cast acrylic block and loading the block as described in the next section.

ELASTIC MODEL PROGRAM

The three-dimensional solid-inclusion borehole probe is in the process of being tested in laboratory models. The initial laboratory model study has been completed and has proved the feasibility of the probe. Measured strain changes in a virtually elastic model have been converted to stress changes.

The laboratory elastic model testing program is partly complete. Two tests have been conducted in which a probe (shown in fig. 2) was employed to determine the stress changes occurring within the cast acrylic model (fig. 5). These measurements were reduced by the mathematical method described on page C19. The results were compared with the stress applied, and the stress changes were predicted by elastic theory (p. C24). The comparison indicated good agreement between the stress calculated from measurements and the stress predicted theoretically.

The elastic model was constructed from a single block of cast acrylic 19 inches high, 13 inches wide, and 12 inches deep. A 2-inch-diameter borehole was drilled 6 inches into the block and the probe was grouted into the hole with a nonfilled epoxy for the first test and with a filled epoxy for the second test (fig. 5). The minimum distance between the surface of the probe and the free-surface boundaries of the block was 5½ probe diameters. These conditions resulted in only partial confinement of the probe by the surrounding acrylic.

Two difficulties were encountered in the first elastic model test:

1. Bubbles as much as 14 millimeters in diameter developed between the drill-hole walls and the epoxy plug as the result of skrinkage of the epoxy during curing. This difficulty was eliminated in the second elastic model by the use of a filled epoxy.
2. Air was entrapped within the second of two layers of epoxy used to cement the probe in the acrylic block. This condition was attributed to the heat generated by a poorly controlled epoxy formulation. This problem was solved by the elimination of the double pour and by using a slower setting epoxy in the second model test.

The elastic model was placed in a 400,000-pound press and loaded axially to 200,000 pounds in the first test and 300,000 pounds in the second test to determine what stress changes occurred in the probe as a result of the loading. One surface of the model was instrumented with strain-gage rosettes for the second test (fig. 5) in order to obtain control information for interpretation of test results.

The elastic model tests have shown close overall agreement with elastic theory. The differences measured have been well within the

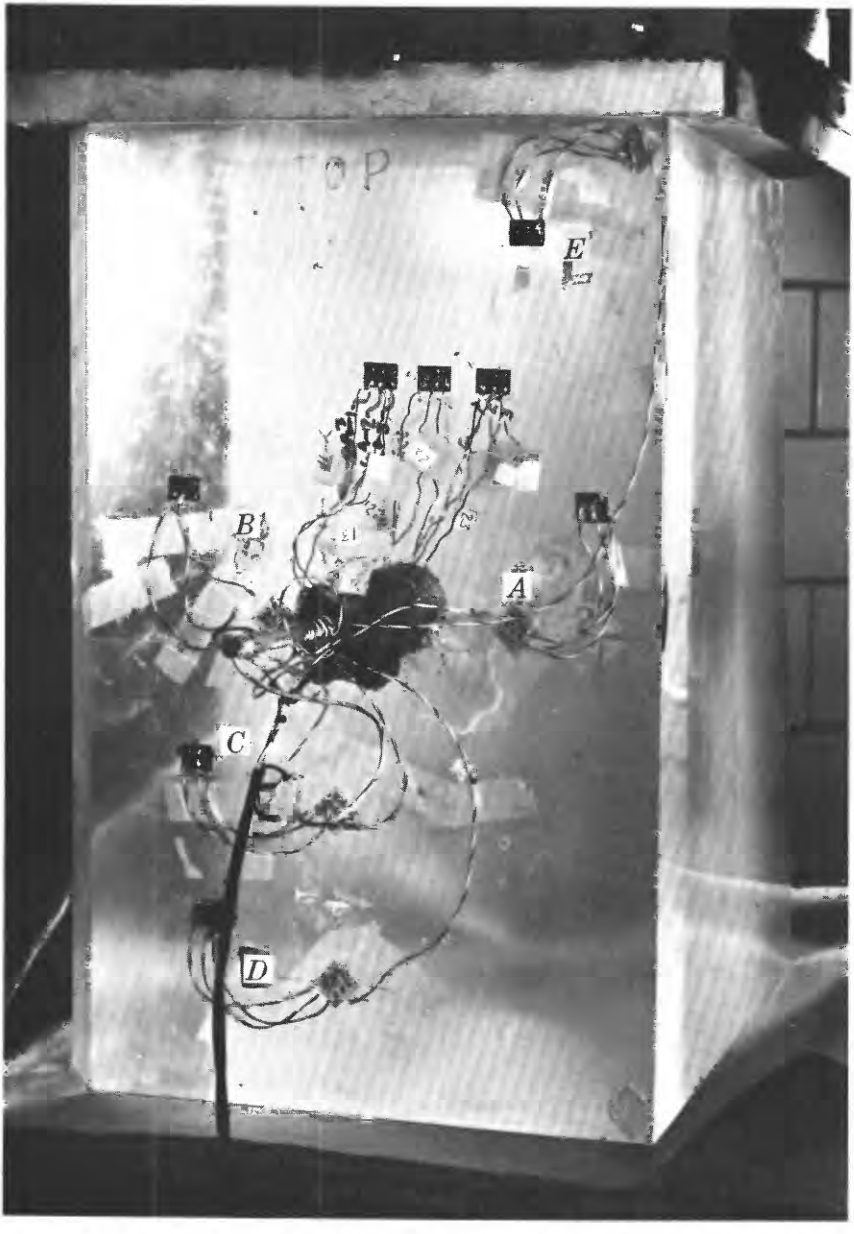

FIGURE 5.—Block of cast acrylic showing three-dimensional borehole probe grouted into central core hole. *A–E*, strain gages on external surface.

variations anticipated as the result of the acrylic block not behaving as a perfectly elastic body. Tensile strains as the result of the Poisson effect, a term used to describe the lateral deformation resulting from longitudinal stress (Coates, 1965, p. B14; Seldenrath and Gramberg, 1958, p. 80–91; and Jenkins, 1958, p. 102), were present in the proper direction and magnitude as theoretically predicted with respect to the physical constants for the acrylic and the applied loading. The principal stress changes were calculated for the two completed tests. The measured surface compressive stress pattern and stress trajectories were then plotted (fig. 8).

FIRST TEST

The results of the first elastic model test indicated that the probe was situated in a triaxial stress field (fig. 6). This stress field is highly directional, and the maximum principal compressive stress change is almost parallel to the applied compressive load. This compressive stress resulted in a lateral strain in all directions in planes normal to the loading direction. Having measured Young's modulus and Poisson's ratio for the acrylic and the epoxy (which were almost identical) and knowing that no external restraint was applied to the model, we were able to predict the tensile stresses which should have been obtained from probe measurements. The lateral stress obtained from probe measurements should have been about 0.39 times the maximum principal compressive stress change for the finite but unrestrained model employed. Because of the bubbles which formed along parts of the drill hole, the lateral stresses obtained from the probe measurements were not equal along and across the drill hole. However, the average value of these stresses indicated a lateral tensile stress of 0.35 times the maximum principal compressive stress change.

The fact that the magnitude of the maximum principal compressive stress change obtained from the probe measurements was twice the applied compressive stress is attributed to the confinement of the probe in the model. It should be remembered that uniaxial compression does not imply uniform compression. This aspect of the model and probe response was investigated as part of the second elastic model test.

SECOND TEST

In the second elastic model test the probe was grouted in place with a metal-filled epoxy having a static Young's modulus of 1.55×10^6 psi compared to the acrylic static modulus of 0.327×10^6 psi. The probe was virtually confined on three sides by acrylic and one one side by the metal-filled epoxy. The principal stress changes which were determined are shown in figure 7. This stress field was also highly directional, and the maximum principal compressive stress change alined

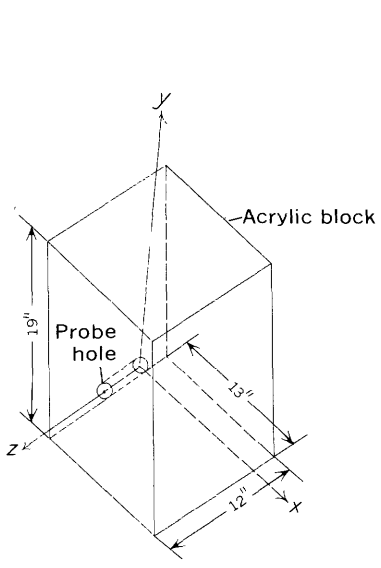

x-axis bears S. 45° E. and plunges 10°
y-axis bears S. 45° W. and plunges 80°
z-axis bears S. 45° W. and is horizontal

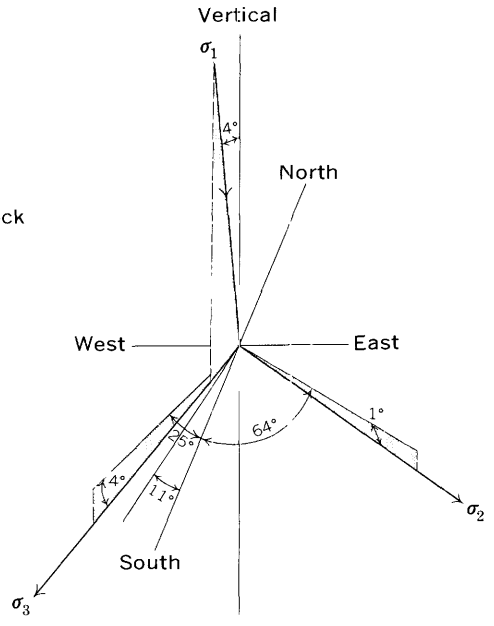

STRESSES ACTING ON PROBE

Principal stress	Magnitude (psi) (+) compression (−) tension	Bearing	Plunge
σ_1 (maximum)	+2640	S. 11° W.	86°
σ_2 (intermediate)	− 113	S. 64° E.	1°
σ_3 (minimum)	−1728	S. 25° W.	4°

FIGURE 6.—Stresses determined from elastic model test 1, under a 200,000-pound load. Vertical planes are stippled.

itself with the applied load. The lateral stresses obtained from probe measurements were influenced by the physical properties of the acrylic block and the filled epoxy grout. Because the grout had a greater stiffness than the acrylic, one of the remaining principal stresses was alined parallel to the drill hole and the other was alined normal to the drill hole. Based on the directional variations of stiffness, theoretical stress calculations were made to check the validity of the lateral stresses obtained from probe measurements (p. C24). The agreement of the theoretically computed stresses and the probe stresses was within 7 percent.

Muskhelishvilis' mathematical plane stress or plane strain analysis of the influence of a circular welded elastic inclusion within an elastic body provides a theoretical means of demonstrating the absence of any

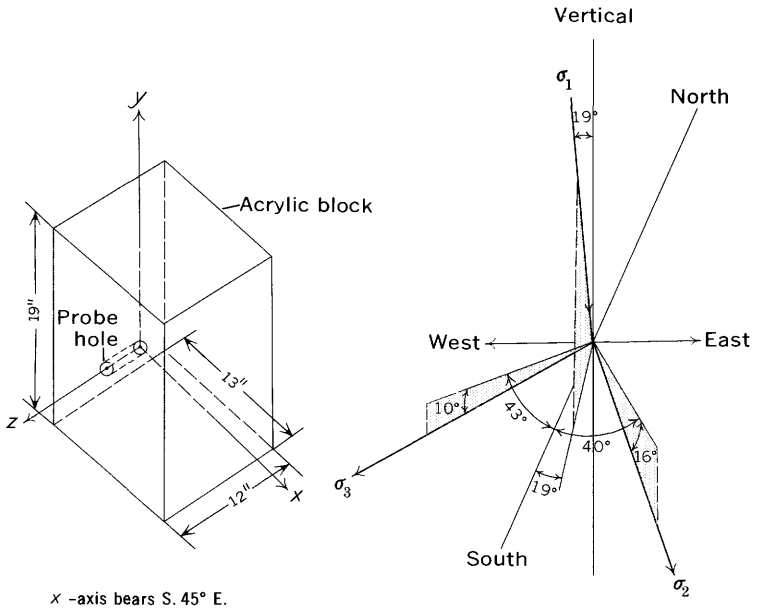

x -axis bears S. 45° E. and is horizontal
y -axis is vertical
z -axis bears S. 45° W. and is horizontal

STRESSES ACTING ON PROBE

Principal stress	Magnitude (psi) (+) compression (−) tension	Bearing	Plunge
σ_1 (maximum)	+3876	S. 19° E.	71°
σ_2 (intermediate)	−1885	S. 40° E.	16°
σ_3 (minimum)	−3610	S. 43° W.	10°

FIGURE 7.—Stresses determined from elastic model test 2, under a 300,000-pound load. Vertical planes are stippled.

stress or strain concentration influences resulting from the borehole in which the probe is placed (Leeman, 1964, p. 54–56). This analogy holds for any such inclusion provided the inclusion is elastic and welded, regardless of the relative stiffness of the inclusion and the host material. (See note facing page C1.)

The field borehole probe has been designed so that in a 3-inch-diameter borehole the stress-carrying member extends on each end at least 7 inches (7 ball diameters) from the center of the probe. When the probe is grouted into a borehole, the stresses contained within the host material are transmitted uniformly through it except at the very ends where stress decay is expected. If the 60° approximation of the Boussinesq stress-influenced zone is used to define the zone surrounding the probe, then a uniform nondecayed stress field would be expected to exist around and beyond the sensing ball. Thus this part of the

probe should act as a solid welded inclusion, nearly perfectly confined, and there should be no effect on the transmitted stresses induced by the geometry of the borehole.

The discrepancies between stresses obtained from measurements in the acrylic block and those calculated from theoretical considerations can be explained by the fact that neither of the theoretical boundary conditions (complete restraint or complete nonrestraint) was effective. The acrylic model block was considerably too narrow to act as a semi-infinite restraining mass to the probe, but was not too narrow (infinitesimal) to offer a certain amount of restraint to the probe. The effectiveness of this restraint in confining the central parts of the model can be seen in figures 7 and 8.

The fact that the stress obtained from probe measurements was double the applied stress in that direction led to the emplacement of the strain-gage rosettes on one surface of the model as described previously. The principal stress trajectories were constructed from the rosette results, and the maximum compressive stress present on that surface of the model was contoured (fig. 8). From these results it can be seen that the size and geometry of the elastic model resulted in increased restraint. This was indicated by high values of compression at the center of the model. Consequently, the load-carrying capacity increased toward the center of the model. The geometry of the model employed in these tests apparently resulted in a stress concentration at the probe location of twice the applied stress. This stress concentration results from the triaxial confinement of the probe by the surrounding acrylic and grout.

MATHEMATICAL ANALYSIS OF PROBE MEASUREMENTS

The strain gages that are attached to the probe measure the induced strains in three directions at each of three positions on the surface of the spherical probe. The three principal stress changes in the rock mass are transmitted to the probe, and each strain gage measures the resultant strain induced in the direction of the gage orientation. Therefore, each strain rosette permits the calculation of the strain ellipse that was produced by all three principal stress changes in the plane of measurement. In addition, the normal stresses on the surface of the sphere in the direction of the strain gages and the shear stresses normal to the direction of the strain gages may be calculated if Young's modulus and Poisson's ratio for the probe are known.

The stresses and strains in the probe are not the same as those in the host material because the relative stiffness of the two materials is very different. Because the probe is virtually rigid, the stress in it will ap-

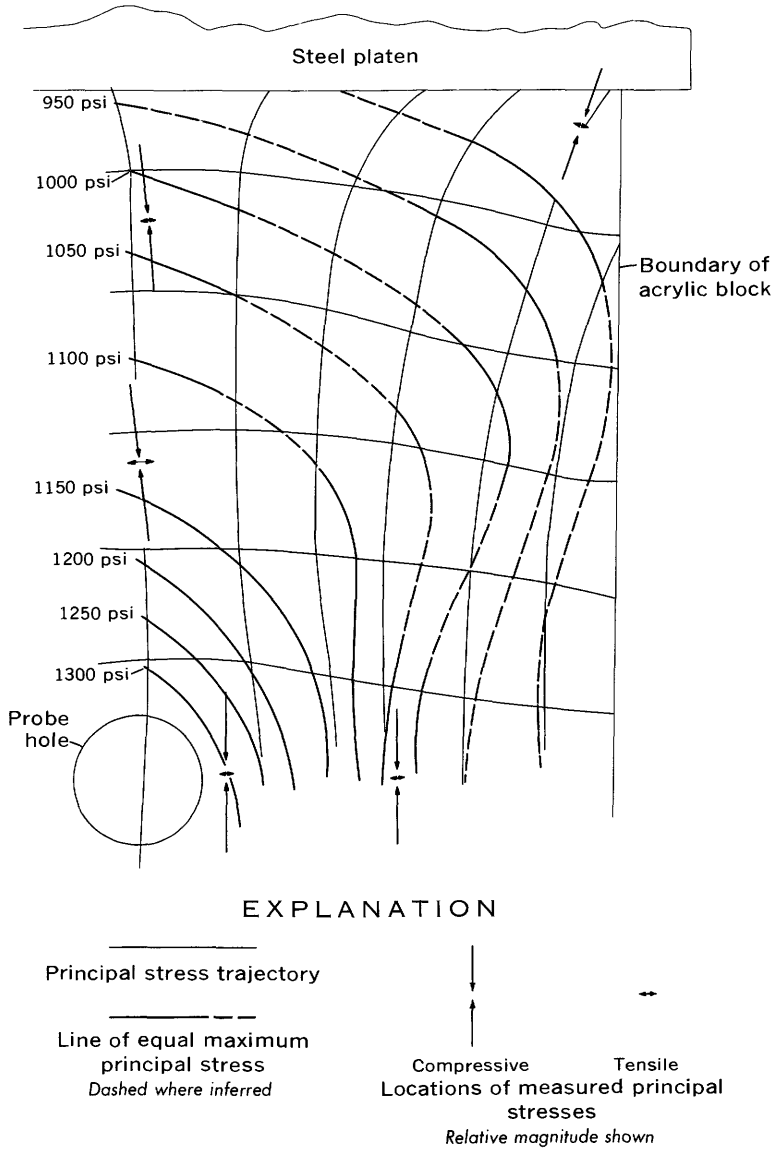

FIGURE 8.—Surface stress on model test 2.

proach the limit of about 1.5 times the stress in the host material (Leeman, 1964, p. 55). (See note facing page C1.)

The calculation of the plane stress or plane strain ellipse from 45° rosette data is a standard stress analysis technique (Hetényi, 1958, p. 412), based on the fact that strain measurements in any three nonparallel directions precisely determine one strain ellipse. Once the stress

ellipse has been calculated, normal and shear stresses can be computed for any direction in the plane of the ellipse. In this study the directions of interest are those parallel to the arbitrary x, y, and z axes of the probe.

After the shear and normal stresses have been calculated (Hetényi, 1958, p. 412) for each of the strain-gage directions on each of the three orthogonal stress ellipses that are parallel to the reference axes, the components of the stress tensor for either the probe or the host material can be calculated. The rosettes produce two stress determinations for each of the three orthogonal normal stresses and one determination of the shearing stress acting in the direction of each of the arbitrary axes, x, y, and z. The duplicate normal stresses are checked for compatibility and are averaged as part of the calculation. The six shearing stresses in the stress tensor are actually only three different shearing stresses, because:

$$\tau_{xy}=\tau_{yx},$$

$$\tau_{xz}=\tau_{zx},$$

and

$$\tau_{yz}=\tau_{zy}.$$

(Note: τ_{xy} is the shear stress on the yz plane parallel to the y axis and normal to x axis.)

The stress tensor is determined by the following stresses:

$$\begin{matrix}\sigma_{xx} & \tau_{xy} & \tau_{xz}\\ \tau_{yx} & \sigma_{yy} & \tau_{yz}\\ \tau_{zx} & \tau_{zy} & \sigma_{zz}\end{matrix}$$

(Note: σ_{xx} is the normal stress acting on the yz plane parallel to the direction of the x axis.) The stress tensor is then solved as a determinant for that set of three orthogonal stresses denoted by S (Sechler, 1952) which, when rotated to a unique position, reduce the shearing stresses to zero.

$$\begin{vmatrix}(S-\sigma_{xx}) & -\tau_{xy} & -\tau_{xz}\\ -\tau_{yx} & (S-\sigma_{yy}) & -\tau_{yz}\\ -\tau_{zx} & -\tau_{zy} & (S-\sigma_{zz})\end{vmatrix}=0$$

The expanded determinant reduces to:

$$S^3-(\sigma_{xx}+\sigma_{yy}+\sigma_{zz})S^2+(\sigma_{xx}\sigma_{yy}+\sigma_{xx}+\sigma_{zz}+\sigma_{yy}\sigma_{zz}-\tau_{xy}{}^2-\tau_{yz}{}^2-\tau_{zz}{}^2)S-(\sigma_{xx}\sigma_{yy}\sigma_{zz}+2\tau_{xy}\tau_{yz}\tau_{zx}-\sigma_{xx}\tau_{yz}{}^2-\sigma_{yy}\tau_{zx}{}^2-\sigma_{zz}\tau_{xy}{}^2)=0, \quad (1)$$

which in turn can be solved for its real roots S_1, S_2, and S_3, the magnitudes of the principal stresses.

The next step in the mathematical analysis is to determine the direction cosines (l_i, m_i, and n_i) of the angles between each of the three principal stress change axes (i) and the reference probe axes (x, y, z). This can be accomplished by substituting the principal stress change values and the normal and shear stress changes determined from the rosettes in the following simultaneous equations (Sechler, 1952, p. 23):

$$(S_i-\sigma_{xx})l_i-\tau_{xy}m_i-\tau_{xz}n_i=0, \quad (2)$$

$$-\tau_{yx}l_i+(S_i-\sigma_{yy})m_i-\tau_{yz}n_i=0, \quad (3)$$

$$-\tau_{zx}l_o-\tau_{zy}m_i+(S_i-\sigma_{zz})n_i=0, \quad (4)$$

and

$$l_i{}^2+m_i{}^2+n_i{}^2=1, \quad (5)$$

where

S_i=respective maximum (1), intermediate (2), or minimum (3) principal stress change;

l_i=direction cosine of the angle between the arbitrary x axis and the i principal stress change axis;

m_i=direction cosine of the angle between the arbitrary y axis and the i principal stress change axis; and

n_i=direction cosine of the angle between the arbitrary z axis and the i principal stress change axis.

After calculating the nine direction cosines, for the angles between the reference (x, y, z) axes and the three principal stress change axes, one must calculate the bearing and plunge of the principal stress change axes. This is accomplished by first calculating the angles between the reference probe axes and the directions north, east, and vertical. This calculation is based on the properties of right spherical triangles. The cosine of the face angle of a right spherical triangle opposite the right diedral angle equals the product of the cosines of

the other two face angles (Kells and others, 1940, p. 271–273). From this the following formulas are derived:

$$l_k = \cos N_j \cos V_j, \tag{6}$$

$$m_k = \cos (90° - V_j), \tag{7}$$

and

$$n_k = \cos E_j \cos V_j, \tag{8}$$

where

j=respective arbitrary x, y, or z axis and
k=respective north (N), vertical (V) or east (E) spatial axis.
l_k=direction cosine of the angle between arbitrary x axis and the respective k spatial axis.
m_k=direction cosine of the angle between the arbitrary y axis and the respective k spatial axis.
n_k=direction cosine of the angle between the arbitrary z axis and the respective k spatial axis.
N_j=horizontal angle between north and j axes.
V_j=vertical angle between horizontal and j axes (downward plunge is positive).
E_j=horizontal angle between east and j axes.

The direction cosines for the angles between the principal stress change axes and the north, east, and vertical axes can then be calculated. This follows from the fact that the cosine of the angle between any two intersecting lines in any three-dimensional system is equal to the sum of the products of their respective direction cosines, as follows:

$$\cos \theta_{ki} = l_k l_i + m_k m_i + n_k n_i, \tag{9}$$

where

θ_{ki}=angle between respective spatial axis—north (N), vertical (V), or east (E)—and respective principal stress change direction—maximum (1), intermediate (2), or minimum (3).

These angles, between directions of the principal stress changes and north, east, and vertical, are then reduced to horizontal and vertical angular components, again by using the properties of spherical triangles with one right angle. The horizontal angle between any principal stress change direction and north is the bearing of that principal stress change, and the complement of the vertical angle is the plunge of that principal stress change.

$$\cos \theta_{Ni} = \cos Ni \cos Vi. \tag{10}$$

$$\cos \theta_{Vi} = \cos (90° - Vi). \tag{11}$$

$$\cos \theta_{Ei} = \cos Ei \cos Vi, \tag{12}$$

where

θ_{Ni}=angle between north axis and the respective i principal stress change axis (1, 2, or 3),
θ_{Vi}=angle between vertical axis and the respective i principal stress change axis (1, 2, or 3),
θ_{Ei}=angle between east axis and the respective i principal stress change axis (1, 2, or 3),
Ni=horizontal angle between north axis and the respective i principal stress change axis (1, 2, or 3),
Vi=vertical angle between horizontal axis and the respective i principal stress change axis (1, 2, or 3) (downward plunge is positive), and
Ei=horizontal angle between east axis and the respective i principal stress change axis (1, 2, or 3).

The last step in the mathematical analysis consists of the determination of the magnitude, bearing, and plunge of the maximum shearing stress changes which accompany the previously calculated principal stress changes.

$$\tau_{max} = (S_1 - S_3)/2, \tag{13}$$

where

S_1=maximum principal stress change,

S_3=minimum principal stress change, and

τ_{max}=maximum shearing stress change.

The preceding calculations have been programed for computer analysis in the interest of economy, speed, and accuracy.

COMPUTATION OF LATERAL STRESSES IN SECOND ELASTIC MODEL TEST

Static testing of the elastic constants of the acrylic block and the partly metal-filled epoxy grout, in addition to an accurate knowledge of the geometric distribution of these materials in the laboratory model, permitted calculation of the effective moduli in any direction. The calculated effective moduli are determined by making a 60° approximation of the Boussinesq stress-influenced zone from the sides

of the spherical probe for each of the stress directions. The maximum principal stress (σ_1) zone has only a small (3/8 inch) annulus of metal-filled epoxy with the remaining 8 5/8 inches on each side in the acrylic. The intermediate principal stress (σ_2) zone has about the same annulus of metal-filled epoxy but only 5 5/8 inches of acrylic on each side. The minimum principal stress (σ_3) zone, which contains the borehole, has a rather complex geometric distribution of metal-filled epoxy and acrylic. This distribution also differs from side to side. Accurate measurement of the geometric material distribution within the 60° stress zone permitted an estimate to be made for the effective elastic modulus in the direction of the minimum principal stress.

Following are the material moduli, Poisson's ratios, and calculated effective elastic moduli:

1. Modulus of the acrylic block$=0.327\times10^6$ psi.
2. Modulus of the filled grout$=1.55\times10^6$ psi.
3. Poisson's ratio (all materials)$=0.39$
4. Effective modulus in the direction of the maximum principal stress, $E_1=0.330\times10^6$ psi.
5. Effective modulus in the direction of the intermediate principal stress, $E_2=0.347\times10^6$ psi.
6. Effective modulus in the direction of the minimum principal stress, $E_3=0.706\times10^6$ psi.

By using these constants, the stress relationships can be calculated as follows:

Assume the principal stresses σ_1, σ_2, or $\sigma_3\neq0$.

Assume the principal strains $\epsilon_1\neq\epsilon_2\approx\epsilon_3\neq0$.

Then by using the relationships from Sechler (1952, p. 55),

$$\epsilon_1=\frac{1}{E_1}\left[\sigma_1-\mu(\sigma_2+\sigma_3)\right],$$

$$\epsilon_2=\frac{1}{E_2}\left[\sigma_2-\mu(\sigma_1+\sigma_3)\right],$$

and

$$\epsilon_3=\frac{1}{E_3}\left[\sigma_3-\mu(\sigma_1+\sigma_2)\right],$$

it can be shown that

$$\sigma_2=-\sigma_1\frac{\mu(E_3-E_2)}{E_3+\mu E_2}+\sigma_3\frac{E_2+\mu E_3}{E_3+\mu E_2}.$$

By substituting the effective moduli and Poisson's ratio, the above relationship can be expressed as follows:

$$\sigma_2 = -0.226\sigma_1 + 1.35\sigma_3, \tag{14}$$

or

$$\sigma_3 = \frac{\sigma_2 + 0.226\sigma_1}{1.35}, \tag{15}$$

or

$$\sigma_1 = \frac{1.35\sigma_3 - \sigma_2}{0.226}. \tag{16}$$

By substituting measured values of σ_1 and σ_3 into equation 14, $\sigma_2 = -2{,}015$ psi of tension compared with the actual measured value of $-1{,}885$ psi of tension. Similarly, σ_3 as computed becomes $-3{,}420$ psi of tension as compared with a measured value of $-3{,}610$ psi of tension.

FIELD INVESTIGATIONS

The laboratory investigations and probe development were, in part, an outgrowth of field studies performed by the U.S. Geological Survey over a period of several years. During the course of these studies, both at the surface and underground, the need for more adequate stress determinations was recognized. For example, in the Straight Creek Tunnel pilot bore (Robinson and Lee, 1964, 1967) the rock load on the steel sets was measured by the contractor with prop-load cells and the deflection of the walls and roof was measured with borehole extensometers. More than 40 instrument stations were established through the 8,350-foot-long bore. This provided a large amount of data on rock behavior during excavation. Nevertheless, very little new knowledge was gained of fundamenetal rock mass behavior. The stress conditions within the rock mass prior to tunneling and the behavior of the stress field in response to tunneling operations are still virtually unknown. The writers believe that a more accurate understanding of these factors will increase the efficiency and economy of underground excavation. For example, in addition to the loads carried by steel sets, it would be helpful in underground mining or tunneling to know the changing state of stress adjacent to the opening and for a considerable distance within the rock surrounding the opening.

Changes in the state of stress adjacent to an active underground opening could be monitored by placing and grouting borehole probes into holes drilled into the walls and ahead of an advancing tunnel face. Further, the state of stress in the rock mass prior to excavation could conceivably be estimated by overcoring the borehole probe.

Other investigators (Varnes, 1962, p. 48) have mentioned the need for a method which would detect the buildup of stresses preceding the development of faults or preceding movement along preexisting faults. Accurate knowledge of the stress buildup in an area would permit the prediction of the possible orientations of fault structures resulting from the indicated stress fields, whether they be related to shear or tensile failure of the rock mass. It should be possible to monitor such a buildup in stress at some distance from a fault because the stresses producing a fault are undoubtedly not restricted in their extent, as faults are not restricted in their extent. It appears feasible, because the probe can be placed at depth in a rock mass, to foresee the use of the probe, in relation to active faults, as a means of predicting impending hazardous movements.

The scarcity of any studies regarding the influence of geologic factors on the distribution of stresses in rock masses makes it imperative that efforts be made to bring about a union between stress analysis and geology in the future of rock mechanics.

REFERENCES CITED

Coates, D. F., 1965, Rock mechanics principles: Canada Dept. Mines and Tech. Surveys, Mines Br. Mon. 874, 338 p.

Dare, W. L., 1962, Measuring changes in pillar strain during pillar recovery—Experiments in a New Mexico uranium mine: U.S. Bur. Mines Rept. Inv. 6056, 17 p.

Edwards, R. H., 1951, Stress concentrations around spheroidal inclusions and cavities: Jour. Applied Mechanics, Am. Soc. Mech. Engineers Trans., v. 73, p. 19–30.

Fitzpatrick, John, 1962, Biaxial device for determining the modulus of elasticity of stress-relief cores: U.S. Bur. Mines Rept. Inv. 6128, 13 p.

Goodier, J. N., 1933, Concentration of stress around spherical and cylindrical inclusions and flaws: Jour. Applied Mechanics, Am. Soc. Mech. Engineers Trans., v. 55, p. 39–44.

——— 1958, Elasticity and plasticity: New York, John Wiley & Sons, Inc., 152 p.

Hast, Nils, 1958, The measurement of rock pressure in mines: Stockholm, Sveriges Geol. Undersökning Årsb., v. 52, no. 3, 183 p.

Hetényi, M., 1958, Handbook of experimental stress analysis: New York, John Wiley & Sons, Inc., 1077 p.

Jenkins, J. D., 1958, Discussion *of* Seldenrath, T. R., and Gramberg, J., Stress-strain relations and breakage of rocks, *in* Walton, W. H., ed., Mechanical properties of non-metallic brittle materials: New York, Interscience Publishers, Inc., p. 102–103.

Kells, L. M., Kern, W. F., and Bland, J. R., 1940, Plane and spherical trigonometry: New York, McGraw-Hill Book Co., 529 p.

Leeman, E. R., 1964, The measurement of stress in rock: South African Inst. Mining and Metallurgy Jour., v. 65, no. 2, p. 45–114.

Merrill, R. H., Williamson, J. V., Ropchan, D. M., and Kruse, G. H., 1964, Stress determinations by flatjack and borehole-deformation methods: U.S. Bur. Mines Rept. Inv. 6400, 39 p.

Morgan, T. A., Fisher W. G. and Sturgis W. J. 1965, Distribution of stress in the Westvaco Trona mine, Westvaco, Wyoming: U.S. Bur. Mines Rept. Inv. 6675, 58 p.

Obert, Leonard, 1962, Effects of stress relief and other changes in stress on the physical properties of rock: U.S. Bur. Mines Rept. Inv. 6053, 8 p.

Obert, Leonard, Duvall, W. I., and Merrill, R. H., 1960, Design of underground openings in competent rock: U.S. Bur. Mines Bull. 587, 36 p.

Panek, L. A., 1966, Calculation of the average ground stress components from measurements of the diametral deformation of a drill hole: U.S. Bur. Mines Rept. Inv. 6732, 41 p.

Panek, L. A., and Stock, J. A., 1964, Development of a rock stress monitoring station based on the flat slot method of measuring existing rock stresses: U.S. Bur. Mines Rept. Inv. 6537, 61 p.

Robinson, C. S., and Lee, F. T., 1964, Geologic research on the Straight Creek Tunnel site, Colorado: Highway Research Board, National Research Council [U.S.], Highway Research Rec. 57, p. 18–34.

———1967, Results of geologic research, Straight Creek Tunnel pilot bore, Colorado: Highway Research Board, National Research Council [U.S.] Highway Research Rec. 185, p. 9–19.

Ryder, J. A., and Officer, N. C., 1965, An elastic analysis of strata movement observed in the vicinity of inclined excavations, *in* Symposium on rock mechanics and strata control in mines: Johannesburg, South African Inst. Mining and Metallurgy Proc., p. 168–193.

Sechler, E. E., 1952, Elasticity in engineering: New York, John Wiley & Sons, Inc., 419 p.

Seldenrath, T. R., and Gramberg, J., 1958, Stress-strain relations and breakage of rocks, *in* Walton, W. H., ed., Mechanical properties of non-metallic brittle materials: New York, Interscience Publishers, Inc., p. 79–102.

Utter, Stephen, 1962, Determination of stresses around an underground opening, Climax molybdenum mine, Colorado: U.S. Bur. Mines Rept. Inv. 6137, 26 p.

Varnes, D. J., 1962, Analysis of plastic deformation according to Von Mises' theory, with application to the South Silverton area, San Juan County, Colorado: U.S. Geol. Survey Prof. Paper 378–B, 49 p.

Wentworth, D. H., 1966, Some factors influencing strain relief overcoring: Golden, Colorado School of Mines, M.S. thesis T–1097, 136 p.

Wisecarver, D. W., Merrill, R. H., Rausch, D. O., and Hubbard, S. J., 1964, Investigation of in situ stresses, Ruth mining district, Nevada, with emphasis on slope design problems in open-pit mines: U.S. Bur. Mines Rept. Inv. 6541, 21 p.

U. S. GOVERNMENT PRINTING OFFICE : 1968 O - 306-521